Thermal Field Desorption Spectroscopy of Chemisorbed Hydrogen for a Single Step Site

N. Ernst,[1] J. H. Block,[1] H. J. Kreuzer,[2] and X. Ye[1],*

[1]*Fritz-Haber-Institut der Max-Planck-Gesellschaft, Faradayweg 4-6, Dahlem, D-14195 Berlin*
[2]*Dalhousie University, Department of Physics, Halifax, Nova Scotia, Canada B3H 3J5*
(Received 11 March 1993)

The steady state molecular hydrogen ion yield from a single atomic step site of a [110]-oriented tungsten and of a [100]-oriented rhodium crystal is determined as a function of surface temperature using mass and energy resolved probe hole field ion microscopy. A second order kinetic model is developed to fit the experimental data thus obtaining the hydrogen binding energy. For local fields of about 3 V/Å the data are close to values obtained from thermal desorption spectroscopy. A comparison is made with calculations of the field-adsorption binding energy of atomic hydrogen on a jellium surface based on density functional theory.

PACS numbers: 68.45.Da, 79.70.+q

Considerable theoretical and experimental work has already been done on the effect of high electrostatic fields [as applied in field ion microscopy (FIM) [1]] on the chemisorption bond of atomic [2,3] and molecular hydrogen [4,5]. On the basis of a relatively simple model a shift to *smaller* binding energies was suggested for chemisorbed hydrogen (H_{ads}) [3]. However, a straightforward measurement of the binding energy of H_{ads} in high electric fields has not been achieved to our knowledge. In this Letter, we describe a novel procedure which allows the determination of local binding energies of H_{ads} for individual step sites of a selected facet of a field emitter tip. Our approach is based on measurements of the local molecular hydrogen ion yield probed at different surface temperatures and analyzed with a second order kinetic model. We first present hydrogen FIM photos and H_2^+ energy distributions taken at low and high temperatures of a tungsten and a rhodium field emitter. An energy diagram for associative thermofield desorption of H_2^+ will

then be discussed to explain present experimental observations. Desorption activation and binding energy E_b data of H_{ads} will be deduced from the comparison of measured and calculated H_2^+ yields from defined surface sites. At the end we compare present E_b values with earlier (field-free) thermal desorption spectroscopy (TDS) data and recent quantum mechanical results which include the effect of the high external electrostatic field.

Figure 1 shows results of (probe hole) FIM observations together with mass-to-charge resolved field ion energy spectroscopy (FIS) of H_2^+. Mass-to-charge resolved retarding potential analyses were performed for ions emitted from a single step site whereby the probed area was less than 10 Å^2 [6]. Retardation curves were differentiated numerically to obtain nondeconvolved H_2^+ energy distributions [7]. In Fig. 1, sections of hydrogen FIM patterns characterize the apex of a [100]-Rh and of a [110]-W tip at relatively low (79 K) and relatively high surface temperatures (above 200 K). The field strengths
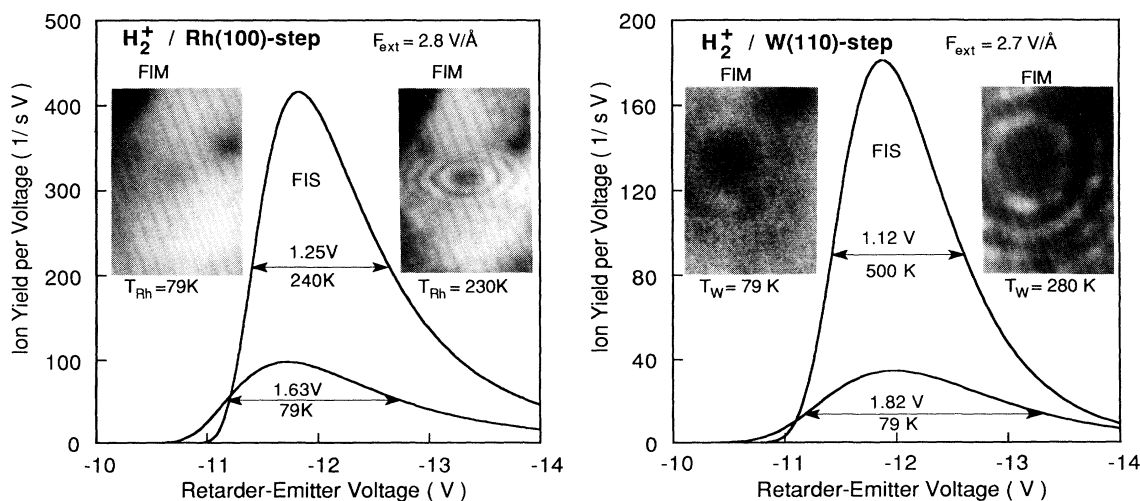

FIG. 1. Hydrogen field ion microscopy (FIM) and field ion energy spectroscopy (FIS) at low and high surface temperatures for [100] rhodium and [110] tungsten. Data were taken at relatively high field strengths above best image conditions at $T_{surface}=79$ K.

at the emitter tips were adjusted above best image fields at 79 K. The calibration of the applied external field F_{ext} was based on standard values for the evaporation field strengths [1]. Local field strength values were derived from H_2^+ appearance energies [8] as will be explained. At $T_{surface} = 79$ K and $F_{ext} \approx 2.7$ V/Å, hydrogen FIM displays less distinct surface features because most H_2^+ and H^+, from field fragmentation of H_2^+, are generated in the gas phase by space field ionization. However, surface features become visible above ca. 200 K. This phenomenon occurs at relatively high fields, approaching the evaporation field strengths at elevated temperatures [9]. This was verified in a recent FIM study on Rh by means of a position sensitive detector [10] suggesting strongly the earlier proposed field enhanced surface diffusion of H_{ads} to plane edge sites [9]. When *surface temperatures* are *raised*, three changes are registered during FIS measurements on H_2^+ for single Rh(100) and for single W(110) step sites. First, the full widths at half maxima (FWHM) of the energy distributions become *smaller*. Second, onsets of H_2^+ energy distributions shift to *increasing appearance energies*. Third, *peak maxima increase* by about a factor of 5.

To explain the experimental results, a scenario is outlined in Fig. 2. The energy diagram introduces some quantities characterizing the thermal field desorption (TFD) of a H_{ads} pair as H_2^+ at a step site. The TFD was detected above $T_{surface} \approx 160$ K for a Rh(100) step and above 240 K for a W(110) step. On the present experimental time scale of minutes, at low surface temperature (79 K) and at constant H_2 pressure (10^{-5} Torr measured in the field-free gas phase away from the tip) there
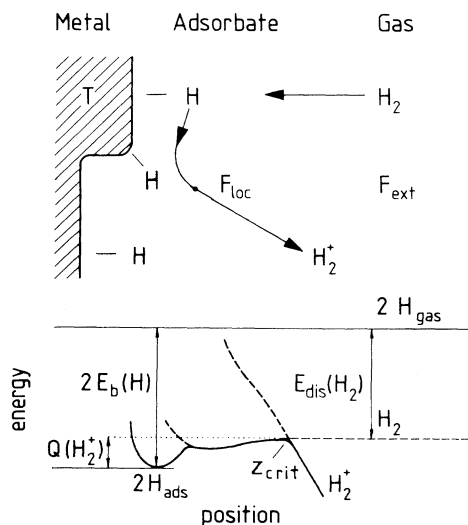

FIG. 2. Model for the thermal field desorption (TFD) of H_2^+ from two H_{ads} at a step site in an externally applied and locally enhanced field characterized by F_{ext} and F_{loc}. The activation energy for TFD is given by $Q(H_2^+)$, determined from the fit of calculated H_2^+ yields to experimental results.

is no significant TFD occurring. The H_2^+ detected under these conditions were most probably generated by field ionization (FI) of relatively high energy H_2 attracted from the gas phase due to polarization forces [1]. Impinging H_2 are field ionized with a high probability at and beyond the critical distance z_{crit}, which is the crossing point of H_2 and H_2^+ interaction curves in Fig. 2 [1,11]. Impinging or hopping molecules, passing z_{crit}, are likely to be ionized after reflection from the surface. The ion energy distribution was recently calculated for such FI processes and is characterized by a relatively broad FWHM [7]. A smaller FWHM was estimated for FI of particles *leaving* the surface with thermal energies, thus explaining our energy spectroscopic results for H_2^+ obtained at higher temperatures.

The appearance energy for a singly charged field ion is given by $A = \Phi_R - e\delta^{on}$, with Φ_R being the work function of the retarding electrode, e being the positive elemental charge, and δ^{on} being the (negative) onset voltage of the ion energy distribution [6,8]. At low surface temperature and at relatively high external field, a significant fraction of H_2 molecules impinging from the gas phase have the full polarization (kinetic) energy in the instant of ionization at z_{crit}, $E_p \approx (\alpha/2) F_{loc}^2$, with α being the polarizability of the molecule. F_{loc} is the local electric field above the step site at $z_{crit} \approx 4$ Å which differs appreciably from F_{ext} at $z \approx 15$ Å [1,12,13]. For such an FI process of gas molecules the appearance energy measures the free-space ionization energy of H_2, $A(79$ K$) \approx I$ [6,13]. During TFD the desorbing molecules preferentially leave the surface in normal direction. Because of the local field gradient desorbing H_2 are slowed down to almost zero kinetic energy in the instant of ionization at z_{crit}, implying $A(> 200$ K$) \approx I + E_p$ [8]. Consequently, the temperature dependent shift of the onset energies is given by

$$e\delta^{on}(79 \text{ K}) - e\delta^{on}(> 200 \text{ K}) \approx (\alpha/2) F_{loc}^2 . \tag{1}$$

Using Eq. (1), values for F_{loc} can be estimated for present experimental conditions, to ca. 3.5 V/Å. This result is in good agreement with earlier theoretical calculations of the field enhancement above an adatom on jellium [12] and recent experimental data showing significantly enhanced field strengths above neon covered step sites of a Rh tip [13].

To determine the activation energy, $Q(H_2^+)$ for TFD, we develop a kinetic model which will allow us to calculate the temperature dependence of the H_2^+ yield and compare it with experimental results. We assume that the ion yield is given by

$$Y(H_2^+) = r_d^+ n_s n_n . \tag{2}$$

In Eq. (2), n_s and n_n are the probabilities that the step (subscript s) and a neighboring site, located on the step or on a terrace (subscript n), are occupied by a hydrogen atom. The thermal desorption rate constant for ions is denoted as r_d^+. The H occupation probability for a step

site changes as a function of time according to

$$dn_s/dt \approx S_s j(1 - n_s) - (r_d^0 + r_d^+)n_s n_n \qquad (3)$$

and a similar equation holds for n_n. Here, j is the flux of particles arriving at the step site or its neighbor site, both from the gas phase and along the surface. Sticking of atoms (originating from molecules previously dissociated at the shaft) occurs with a probability S, provided the site is empty given by a probability $(1 - n)$. If mostly molecules were to arrive at the site and sticking is not precursor mediated, then S should contribute another factor $(1 - n)$. Such differences in the adsorption term have only a minor effect on the parameters in the fit to experimental data. The terms proportional to $n_s n_n$ describe desorption as neutral molecules or molecular ions. Field enhanced surface diffusion is much faster than adsorption and desorption and can thus be ignored in the rare equations.

The desorption rate constant for molecules as neutrals (superscript 0) from an atomic adsorbate is given by [14]

$$r_d^0 = (S_0 a_s 2\pi m_{H_2} k_B^2 T^2 / h^3)$$
$$\times (T/2T_{rot}^0)[q_{vib}^0/(q_3^0)^2]e^{-Q^0/k_B T}. \qquad (4)$$

A similar equation holds for ions (superscript $+$). S_0 is the sticking coefficient (at zero coverage, i.e., equal to 1), a_s is the area of a surface site, and $T_{rot}^{0,+}$ are the rotational temperatures of the neutral (superscript 0) or ion (superscript $+$), respectively. In the vibrational partition functions

$$q_{vib}^{0,+}(T) = \tfrac{1}{2}\sinh(T_{vib}^{0,+}/2T), \qquad (5)$$

$T_{vib}^{0,+}$ are the vibrational temperatures of the neutral or ionized molecule. q_3 consists of three factors like Eq. (5) accounting for the atom-surface vibrations. Activation energies for associative desorption, $Q^{0,+}$, are in general different for neutral and ionized molecules. Good fits

to experimental results were obtained with $Q^0 \approx Q^+$ $=Q(H_2^+)$. The relation to the binding energy E_b of H_{ads} on the surface and the molecular dissociation energy $E_{dis} = 4.47$ eV for gaseous H_2, is approximately given by (Fig. 2)

$$Q(H_2^+) \approx 2E_b - E_{dis}. \qquad (6)$$

Lateral interactions in the adsorbate, a (presumably small) temperature dependence of j, and a relatively small effect of the field on E_{dis} are neglected in this simple model. To get the ion yield we look at stationary solutions [Eq. (3)], $dn_s/dt = dn_n/dt = 0$, with $n_s = n_n = \theta$ and $S_s = S_n = S$. We get for the coverage

$$\theta = -\tfrac{1}{2}[Sj/2(r_d^0 + r_d^+)]$$
$$+ \{\tfrac{1}{4}[Sj/2(r_d^0 + r_d^+)]^2 + [Sj/2(r_d^0 + r_d^+)]\}^{1/2}. \qquad (7)$$

Temperature dependences of the ion yield can thus be calculated from $Y(T) = r_d^+(T)(\theta[r_d^0(T), r_d^+(T)])^2$ using Eqs. (2), (4), and (7).

Differential changes of experimental and theoretical TFD H_2^+ yields dY/dT are plotted as a function of surface temperature in Fig. 3 for a rhodium and a tungsten step site. During the mass and energy resolved probe-hole analysis the surface temperature was scanned with a relatively small velocity of about 0.5 K/sec in order to establish stationary conditions. The measured H_2^+ yields $Y(T)$ originate from a small volume (< 6 Å^3) above the critical surface at the step site. The experimental $Y(T)$ data were smoothed and then differentiated numerically after which theoretical curves of dY/dT were fitted to their maxima. The fits sensitively depended on the activation energy $Q(H_2^+)$ and the atom-surface vibrational frequency of H_{ads}. Because the latter is not well known experimentally, it was varied between 252 cm^{-1} and 1510 cm^{-1} resulting in some uncertainty in the determination of the desorption activation and binding ener-
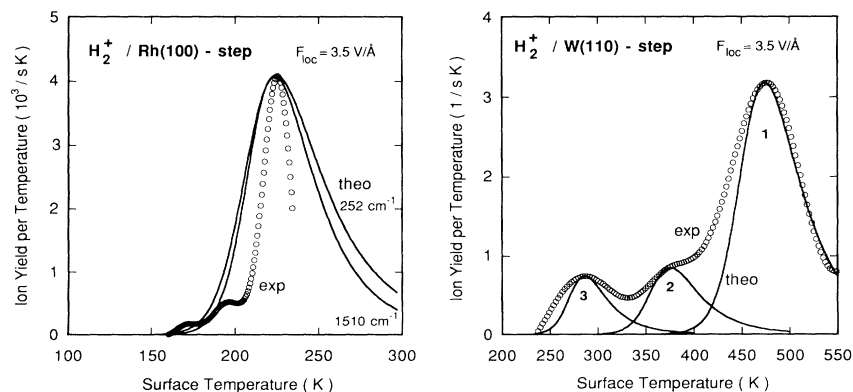

FIG. 3. Differential changes of experimental (circles) and theoretical (lines) H_2^+ yields dY/dT, for individual Rh(100) and W(110) steps. Theoretical data were calculated following Eqs. (2)-(7): $S_0 = 1$, $a_s = 5$ Å^2, $T_{rot}^0 = 85$ K, $T_{rot}^+ = 43$ K, $T_{vib}^0 = 6332$ K, $T_{vib}^+ = 3341$ K (for Rh and W), $T_{vib}(H_{ads}) = 363$-2173 K (252-1510 cm^{-1}), $Q^0 = Q^+ = 0.3$-0.8 eV for Rh, and $T_{vib}(H_{ads}) = 1170$ K, $Q^+ = 1.4$ eV (1), $Q^+ = 1.2$ eV (2), $Q^+ = 1.0$ eV (3) for W.

TABLE I. Desorption activation and binding energies.

Substrate	F_{ext} (V/Å)	F_{loc} (V/Å)	$Q(H_2^+)$ (eV)	$E_b(H)$ (eV)
W(110) [a]	0	0		2.95
				2.84
W(110) step [b]	2.7	3.5	1.3 ± 0.1	2.9 ± 0.1
			1.05 ± 0.15	2.75 ± 0.1
			0.85 ± 0.15	2.65 ± 0.1
Rh(100) [a]	0	0		2.64
Rh(100) step [b]	2.8	3.5	0.55 ± 0.25	2.6 ± 0.2
Jellium [c]	0		1.35	2.91
	3–4		0.5–0.3	2.5–2.3

[a]TDS [W(110), Ref. [15], Rh(110), Ref. [16]].
[b]TFD (this work).
[c]$r_s = 1.058$ Å (Ref. [17]).

gies. Variation of the local adsorption rate constant, Sj, did not have a significant effect on Q data but did determine the actual height of calculated TFD peaks which were fitted to the experimental results.

In Table I we summarize our TFD results. Within error bars, H binding energies in the presence of an external field of 2.7 V/Å agree with numbers derived from field-free thermal desorption spectroscopy (TDS) [15,16]. For the W(110) step, two well pronounced low temperature peaks indicate binding states having smaller energies, at least within the framework of our present model. Recent results of self-consistent jellium calculations [17] (both with and without external field) are in good agreement with the TFD data on the Rh surface, but do not compare as well for adsorption on a tungsten surface for which a jellium model is much more dubious in any case because of more complex electronic structure. It is clear that a more quantitative theoretical understanding can only come about after local site geometry and band structure effects are taken into account.

In conclusion, we have presented a novel method for evaluating binding energy data of chemisorbed hydrogen atoms in high electrostatic fields analyzing thermally field desorbed H_2^+ yields for individual step sites. Our present results are close to data known from field-free experiments on macroscopic single crystal surfaces, at least for W(110) and Rh(100). Earlier and recent theoretical estimates are supported suggesting only a relatively small reduction of the hydrogen chemisorption bond for field strengths of about 3 V/Å. Further experimental and theoretical work is certainly left to be done, such as on the origin of the structures on the low temperature side of

differential yield curves, detected, for example, in the case of tungsten below 300 K.

*Present address: Department of Chemistry, The University of British Columbia, Vancouver, British Columbia, Canada V6T 1Z1.

[1] E. W. Müller and T. T. Tsong, Field-Ion Microscopy (Elsevier, New York, 1969); Prog. Surf. Sci. 4, 1 (1973); E. W. Müller, in Methods of Surface Analysis, edited by A. W. Czanderna, Methods and Phenomena Their Applications in Science and Technology Vol. 1 (Elsevier, Amsterdam, 1975), p. 329.

[2] J. R. Smith, S. C. Ying, and W. Kohn, Phys. Rev. Lett. 30, 610 (1973).

[3] M. Hellsing and B. Hellsing, Surf. Sci. 176, 249 (1986).

[4] G. L. Kellogg, J. Chem. Phys. 74, 1479 (1981); in this study a preliminary value for a field independent desorption activation energy for hydrogen on molybdenum was reported.

[5] W. Drachsel and J. H. Block, Surf. Sci. 246, 141 (1991).

[6] N. Ernst, Appl. Surf. Sci. 67, 82 (1993).

[7] N. Ernst, G. Bozdech, H. Schmidt, W. A. Schmidt, and G. L. Larkins, Appl. Surf. Sci. 67, 111 (1993); deconvolution reduces FWHM data in Fig. 1 by about 0.2 eV.

[8] R. G. Forbes, Surf. Sci. 61, 221 (1976).

[9] N. Ernst and J. H. Block, Surf. Sci. 126, 397 (1983).

[10] W. Miller, Ph.D. thesis, Freie Universität Berlin, 1990.

[11] T. Sakurai, T. T. Tsong, and E. W. Müller, Phys. Rev. B 10, 4205 (1974).

[12] H. J. Kreuzer, L. C. Wang, and N. D. Lang, Phys. Rev. B 45, 12050 (1992).

[13] W. A. Schmidt, N. Ernst, and Y. Suchorski, Appl. Surf. Sci. 67, 101 (1993).

[14] See, e.g., H. J. Kreuzer and S. H. Payne, in Dynamics of Gas-Solid Collisions, edited by C. T. Rettner and M. N. R. Ashford (Royal Society of Chemistry, Cambridge, 1991).

[15] P. W. Tamm and L. D. Schmidt, J. Chem. Phys. 54, 4775 (1971).

[16] M. Ehsasi and K. Christmann, Surf. Sci. 194, 172 (1988); for a review of hydrogen surface interactions, see K. Christmann, Surf. Sci. Rep. 9, 1 (1988).

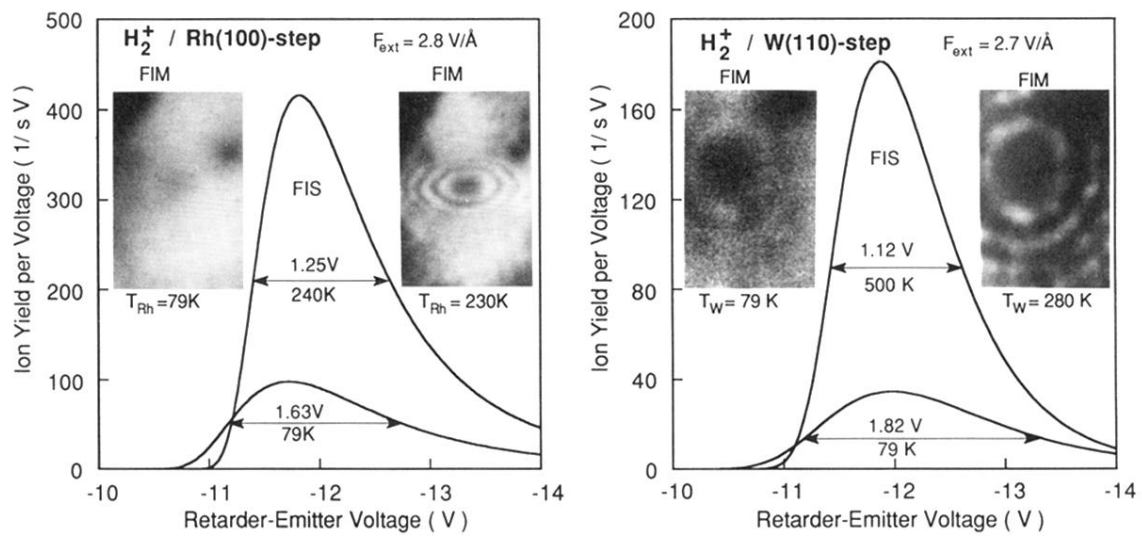[17] X. Ye, H. J. Kreuzer, and D. R. Salahub, Appl. Surf. Sci. 67, 1 (1993).

FIG. 1. Hydrogen field ion microscopy (FIM) and field ion energy spectroscopy (FIS) at low and high surface temperatures for [100] rhodium and [110] tungsten. Data were taken at relatively high field strengths above best image conditions at $T_{surface} = 79$ K.